

Detection of *Ureaplasma urealyticum* by Catalytic Hairpin Assembly Combined with a Lateral Flow Immunoassay Strip

Feng Xiao,[†] Qingrong Qu,[†] Mingyuan Zou, Feiya Su, Huina Wu, Yan Sun, Meiling Zhou, Fengfeng Zhao, Yuming Yao, Gulinaizhaer Abudushalamu, Yaya Chen, Chen Zhang, Xiaobo Fan,* and Guoqiu Wu*



Cite This: *ACS Omega* 2022, 7, 33830–33836



Read Online

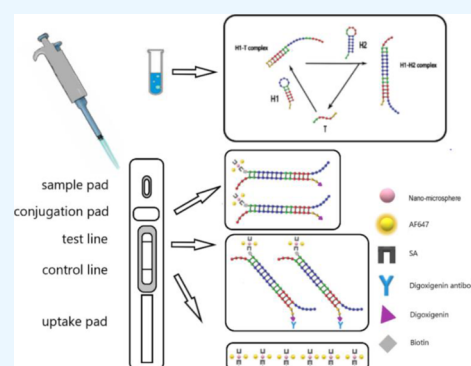
ACCESS |

Metrics & More

Article Recommendations

Supporting Information

ABSTRACT: *Ureaplasma urealyticum* is a common genital mycoplasma in men and women, which can cause reproductive tract infection and infertility, and is also related to adverse pregnancy outcomes and neonatal diseases. Pathogen culture and polymerase chain reaction (PCR) are the main methods for the diagnosis of *U. urealyticum*. However, pathogen culture takes too long, and PCR requires professional personnel and sophisticated instruments. Here, we report a simple, convenient, sensitive, and specific detection method, which combines catalytic hairpin assembly with a lateral flow immunoassay strip. Only a water bath and a fluorescence reader are needed to detect the results in 30 min. We can realize the point-of-care testing of *U. urealyticum* by this method. To verify this method, we selected 10 clinical samples for testing, and the test results were exactly the same as the clinical report.



1. INTRODUCTION

Ureaplasma urealyticum is a particular bacterium with no cell wall. It has 14 known serotypes and is divided into two biotypes—*U. urealyticum* and *Ureaplasma parvum*. *U. urealyticum* has several genes that encode surface proteins, the most important of which is the gene encoding multiple banded antigen (MBA). The C-terminal domain of MBA has antigenicity and can cause a host antibody response. Other virulence factors include phospholipase An and C, IgA protease, and urease.¹ It has been reported that the total infection rate of mycoplasma of 4082 patients with urogenital tract infection in China is 38.39%, mainly infected by single *U. urealyticum*,² which is inconsistent with some research results.^{3–5} It suggests that there are some differences in the distribution of mycoplasma in different areas. It may be related to the different levels of antibiotic use, sampling sites, detection reagents, and laboratory precision in different regions. The genome of *U. urealyticum* is small, with only 580,000 base pairs, and is attached to the mucosa of the genitourinary tract in adults or in the respiratory tract of infants.⁶ *U. urealyticum* can result in male nongonococcal urethritis (NGU) and infertility⁷ and lead to preterm delivery, infertility, and genital discomfort in women. It is more harmful to newborns, will lead to congenital pneumonia, bronchopulmonary dysplasia, meningitis, and even perinatal death.⁸

At present, the main methods for clinical detection of *U. urealyticum* are pathogen culture method, immunoassay, and polymerase chain reaction (PCR). The pathogen culture method for the detection of *U. urealyticum* is not only the

traditional etiological detection method but also the golden standard for *U. urealyticum* detection. This way costs 2 to 3 days with the need of a special culture medium and culture room, so it is difficult and time-consuming. This method is easily affected by the amount of samples, delivery time, and other factors, such that it may lead to false negative. The immunoassay is not difficult, but the specificity and sensitivity are not ideal. The conventional immunoassay methods include immunospot and enzyme-linked immunosorbent assays. Both methods detect antigens of *U. urealyticum*. The immunospot method was accomplished within 2.5 h with a LOD of 30 ng/mL. The enzyme-linked immunosorbent assay for the membrane antigens was accomplished within 4 h with a LOD of 0.4–1.6 $\mu\text{g/mL}$. The reported specificity and sensitivity were 85 and 94%, respectively.^{9,10} The PCR method has high sensitivity and specificity, but it needs special technical personnel and specific requirements for instruments, so it cannot be popularized in grass-roots units and remote areas. New detection methods are also being developed, such as loop-mediated isothermal amplification (LAMP) method,¹¹

Received: April 21, 2022

Accepted: September 5, 2022

Published: September 15, 2022



droplet digital PCR,¹² and high-throughput multiple gene detection system.¹³

Catalytic hairpin assembly (CHA) is an isothermal non-enzyme nucleic acid signal amplification system. It was originally reported by YIN.¹⁴ In this process, a single-stranded toehold site that neighbors a double strand helix mediates strand displacement with another longer single-stranded oligonucleotide.¹⁵ Two groups of complementary probes with a hairpin structure were designed according to the target fragments for detection. When the target fragment does not exist, both groups of probes remain intact. In the presence of the target fragment, the first process will be triggered. Once the first step was finished, the second toehold in H1 beyond the 5'-end of the target was exposed. In the presence of H2 in the solution, the second step was triggered to release the target. The released target was recycled in this process, further amplifying the fluorescence signal.¹⁶ In this system, the target fragment is replaced in the process of reaction and can enter the next round of reaction again. The reaction principle is shown in Figure 1. Therefore, the goal of target fragment detection can be achieved by detecting double strands.

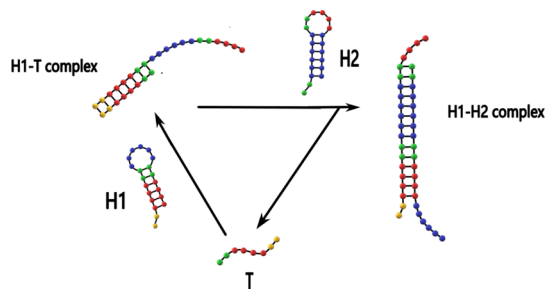


Figure 1. Principle of CHA. $T + H1 \rightarrow H1-T$ complex and $H1-T$ complex + $H2 \rightarrow H1-H2$ complex + T .

We reported a detection method using an isothermal non-enzyme signal amplification system combined with immunoassay strips, which has been successfully applied for the detection of viruses^{17,18} and is now being attempted to be applied to bacteria. Here, we use it to detect *U. urealyticum*. This method does not need complicated preparation or PCR detection equipment and can detect *U. urealyticum* in 30 min. It can detect *U. urealyticum* quickly, cheaply, and sensitively, so it can realize the point-of-care testing of *U. urealyticum*.

2. MATERIALS AND METHODS

2.1. Chemical Materials and Samples. The oligonucleotides used in this study were synthesized and purified by Sangon Biotech. Co., Ltd. (Shanghai, China) (HPLC). Native PAGE gel is purchased from Sangon Biotech. Co., Ltd. (Shanghai, China). The prepared probe is dissolved in TNAK buffer (20×10^{-3} mol/L Tris, pH 7.5; 40×10^{-3} mol/L NaCl; 5×10^{-3} mol/L KCl), annealed, is placed in a water bath at 95 °C, and naturally cooled to room temperature, so that the probe maintains the hairpin structure and then, the probe is placed at -20 °C for standby. All clinical samples were taken from Zhongda Hospital affiliated to Southeast University. A fluorescence detection device for CHA-lateral flow immunoassay strip (LFIA) is GETEIN 1100, purchased from Getein Biotech Inc. (Nanjing, China).

2.2. Genomic Sequence of *U. urealyticum*. The whole genomic sequence of *U. urealyticum* was derived from the

NCBI gene bank (<https://www.ncbi.nlm.nih.gov/>), and MAFFT version 7 (<https://mafft.cbrc.jp>) was used to select multiple sequence alignments. The conservative sequence of *U. urealyticum* was selected in this way. Then, BLAST (<https://blast.ncbi.nlm.nih.gov/>) was used to compare with other bacterial sequences to ensure the specificity of the selected sequence. Finally, NUPACK (<http://www.nupack.org/>) software package is used to design the probe.

2.3. Native Polyacrylamide Gel Electrophoresis. The feasibility of CHA reaction was verified by 12% native polyacrylamide gel electrophoresis. The reagent was reacted at 35 °C for 10 min, then electrophoretic at 110 V for 1 h at room temperature, stained with 10 mg/mL ethidium bromide for 15 min, and the results were observed in an imaging system with 280 nm's ultraviolet wavelength.

2.4. Optimization of CHA Reaction Conditions.

2.4.1. Temperature Optimization. The optimal temperature was detected by real-time fluorescence PCR. The fluorescent group (6-FAM) and quenching group (BHQ1) were labeled on the probe H2. H2 is synthesized and purified by Sangon Biotech (Shanghai) Co., Ltd. 10 μ L 1 μ M H1, 10 μ L 1 μ M H2, and 10 μ L 1 μ M Target were taken as the experimental group, and 10 μ L 1 μ M H1, 10 μ L 1 μ M H2, and 10 μ L 1 μ M TNAK as the control group. The fluorescence signal was measured every 30 s in 15 min with a thermal cycler (CFX96, biorad, America). The reaction temperature was 25, 30, 35, 40, 45, 50, 55, and 60 °C, respectively, and the temperature with the highest ratio of fluorescence intensity between the experimental group and the control group was selected as the reaction temperature.

2.4.2. Proportion Optimization. At the optimum temperature, the reaction ratio of H1:H2 was changed to 1:4, 1:3, 1:2, 1:1, 2:1, 3:1, and 4:1. We added TNAK to keep the total volume unchanged. The control group was set up in each group. The fluorescence signal was measured every 30 s in 15 min with a thermal cycler (CFX96, biorad, America). The proportion with the highest ratio of fluorescence intensity between the experimental group and the control group was selected as the best ratio between H1 and H2.

2.4.3. Concentration Optimization. At the optimum temperature and ratio, the optimal concentrations of H1 and H2 were adjusted by CHA combined with a lateral flow immunoassay (LFIA) strip. The concentration of H1 and H2 was 1, 5, 10, 25, and 50 nM, respectively. The concentration of the Target did not change, keeping it 100 pM. 50 μ L H1, 25 μ L H2, and 25 μ L Target were added. After heating in the water bath, 80 μ L mixed liquid was dropped into the LFIA test strip to determine the fluorescence intensity. The control group was set for each concentration. The concentration with the highest ratio of fluorescence intensity between the experimental group and the control group was selected as the reaction concentration.

2.5. Specificity of CHA-LFIA. Under the optimal reaction conditions, we investigated the effect of sequence error pairing to detection results. In this test, 50 μ L H1, 25 μ L H2, and 25 μ L test sequences were added. After heating in a water bath, 80 μ L mixed liquid was dropped into the LFIA test strip to determine the fluorescence intensity. The fluorescence results of single base mismatch and double base mismatch were compared with the results of perfectly matched base sequence and blank control. Through this way we can judge the specificity of this method.

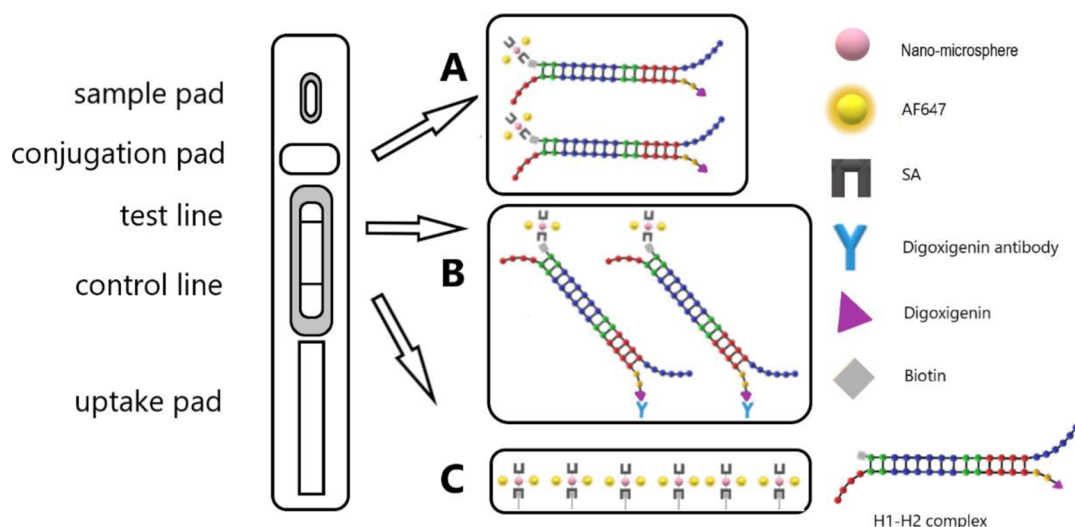


Figure 2. Principle of CHA-LFIA. In the sample pad, H1 (labeled with digoxin) hybridizes with H2 (labeled with biotin) in the presence of the target sequences. H1–H2 complexes bind to double labeled nano–microspheres (labeled with fluorescein Alexa Fluor 647 and streptavidin) through biotin–streptavidin interaction in the conjugation pad (A). The yielded products next bind with the anti-digoxin antibodies immobilized at the test line through hairpin H1 labeled with digoxin (B). At the control line, the excess double labeled nano–microspheres bind with immobilized biotin (C).

2.6. Sensitivity of CHA-LFIA. Under the optimal reaction conditions, different concentrations of target were detected to obtain the detection limit of the CHA-LFIA system. In addition, in the previous experiment, we used TNak buffer. However, in the real clinical samples, there are many other substances, such as proteins, nucleic acids, cells, and so on, which may affect our test results. Therefore, in the sensitivity test, we choose to add the Target to the vaginal secretion swab solution of healthy people, so as to reach the standard of the simulated sample. 50 μL H1, 25 μL H2, and 25 μL Target were added. After heating in a water bath, 80 μL mixed liquid was dropped into the LFIA test strip to determine the fluorescence intensity. The target concentration we selected was 0, 100 aM, 1 fM, 10 fM, 100 fM, 1 pM, 10 pM, 100 pM, and 1 nM.

2.7. Detection of Clinical Samples. Ten clinical samples were selected for detection. Among them, five cases were positive for *U. urealyticum* by PCR, and the other five cases were negative. We detect all samples by CHA-LFIA. We added lysis buffer (50 mM Tris–HCl, 150 mM KCl) to the sample, shook fully, and boiled for 10 min. (13,000 rpm) For 5 min it was centrifuged, then got the supernatant. 50 μL H1, 25 μL H2, and 25 μL supernatant were added. After heating in a water bath, 80 μL mixed liquid was dropped into the LFIA strip to determine the fluorescence intensity. Each group of samples was tested four times, and the data was recorded and compared with the results of PCR.

3. RESULTS AND DISCUSSION

3.1. Principle of CHA-LFIA. We combine the sensitivity of CHA with the simplicity of the LFIA strip, and the detection principle is shown in Figure 2. The binding pad is coated with fluorescein Alexa Fluor 647 and double labeled nano–microspheres with streptavidin (SA), and the nitrocellulose film is marked with a detection line and a quality control line. The detection line is prepared by spraying anti-digoxin/digoxin monoclonal antibody, and biotin is fixed on the quality control line. H1 is labeled with digoxin at the 5' end and H2 with biotin at the 5' end. In theory, when there is no Target, the two probes maintain a stable hairpin structure and will not be

assembled, as shown in Figure 3. When the Target exists, it opens the structure of H1 and exposes more sites, thus

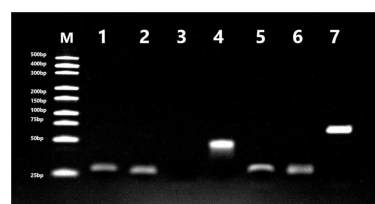


Figure 3. Results of native polyacrylamide gel electrophoresis. Lanes 1: H1; lane 2: H2; lane 3: T; lane 4: H1 + T; lane 5: H2 + T; lane 6: H1 + H2; lane 7: H1 + H2 + T; and M: marker. H1, H2, and T were maintained at a concentration of 100 nM and loaded with 10 μL for gel electrophoresis.

continuing to react with H2 to form a H1–H2 complex. This reaction will replace T and continue to cycle. This reaction was very rapid and a large number of H1–H2 complexes were produced in a short time. We detect H1–H2 to confirm the existence of the target and to know whether there is a corresponding pathogen. The H1–H2 complex forms fluorescent nanospheres through biotin–streptavidin on the binding pad and flows forward continuously. On the detection line, they bind to anti-digoxin antibodies, thus showing fluorescence. Particles that do not form a complex move forward and are captured by biotin as they flow through the quality control line. The fluorescence detection device is used to detect fluorescence, and the difference of fluorescence intensity between the two lines is judged to decide whether there is *U. urealyticum* in the sample. Finally, the absorption pad absorbs the excess liquid.

3.2. Sequence Design. Target, H1, and H2 are used in native polyacrylamide gel electrophoresis; Target, H1, and 6-FAM-H2-BHQ1 are used in real-time fluorescence PCR; and Target, Dig-H1, and Bio-H2 are used in CHA-LFIA (Table 1).

3.3. Native Polyacrylamide Gel Electrophoresis. As shown in Figure 3, both H1 and H2 are a single band, and the Target has run out because its molecular weight is too small.

Table 1. Single Strand DNA Sequences for CHA^a

DNA strands	sequence (5'-3')
Target	CTGTGGCAGCTTCATGTTCTAG
H1	CTAGAACATGAAGCTGCCACAGTCCACGCACCTCTGTGGCAGCTTCA
H2	TGCCACAGAGGTGCGTGGACTGTGGCAGCTTCATCCACGCACCT
Dig-H1	Dig-CTAGAACATGAAGCTGCCACAGTCCACGCACCTCTGTGGCAGCTTCA
Bio-H2	Bio-TGCCACAGAGGTGCGTGGACTGTGGCAGCTTCATCCACGCACCT
6-FAM-H2-BHQ1	6-FAM-TGCCACAGAGGTGCGTGGACTGTGGCAGCTTCATCCACGCACCT-BHQ1
SMT	CTGTGGCAGCTTCATGTTCTAG
DMT	CTGTGTCAGCTTCATGTTCTAG

^aSMT: single mismatched target and DMT: double mismatched target.

Lane 6 is caused by the overlap of H1 and H2 and lane 4 is the H1-T band. Lane 5 is H2 and there are no other bands, indicating that H2 does not react with the Target. Lane 7 is H1-H2 complex.

3.4. Optimization of CHA Reaction Conditions.

3.4.1. Temperature Optimization. The result is shown in Figure 4. The fluorescence intensity of the experimental group/control group is the highest at 35 °C. These results are similar to that of Wu's.¹⁹

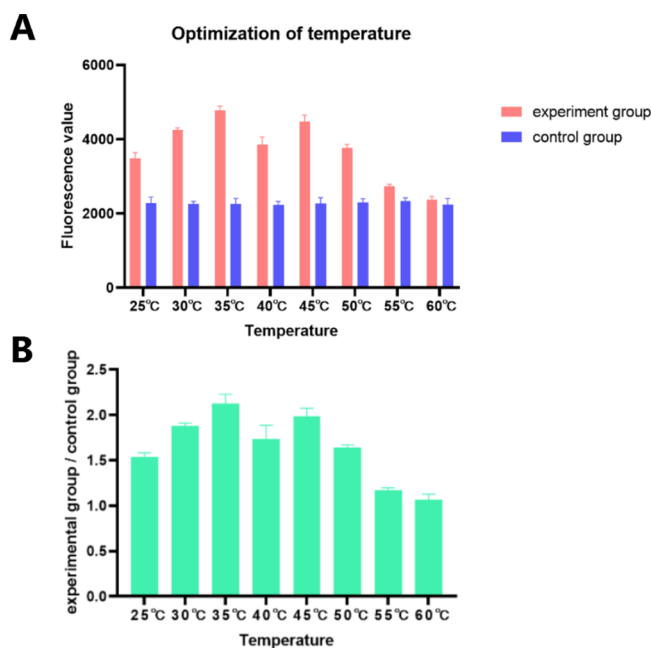


Figure 4. Temperature optimization by real-time fluorescence PCR. (A) Fluorescence values of different temperatures and (B) fluorescence intensity ratio of the experimental group to the control group. The fluorescence values of the experimental group and the control group were detected at different temperatures (25, 30, 35, 40, 45, 50, 55, and 60 °C). Each value was derived from three independent detections, and the error bars mean standard deviations. The fluorescence intensity ratio of the experimental group to the control group was the highest at 35 °C. The concentrations of H1, H2, and Target are all 1 μ M.

3.4.2. Proportion Optimization. The result is shown in Figure 5. We chose H1/H2 = 2:1 as the best ratio. At this time, the fluorescence intensity of the experimental group/control group was the highest.

3.4.3. Concentration Optimization. The result is shown in Figure 6. When the concentrations of H1 and H2 were both 10

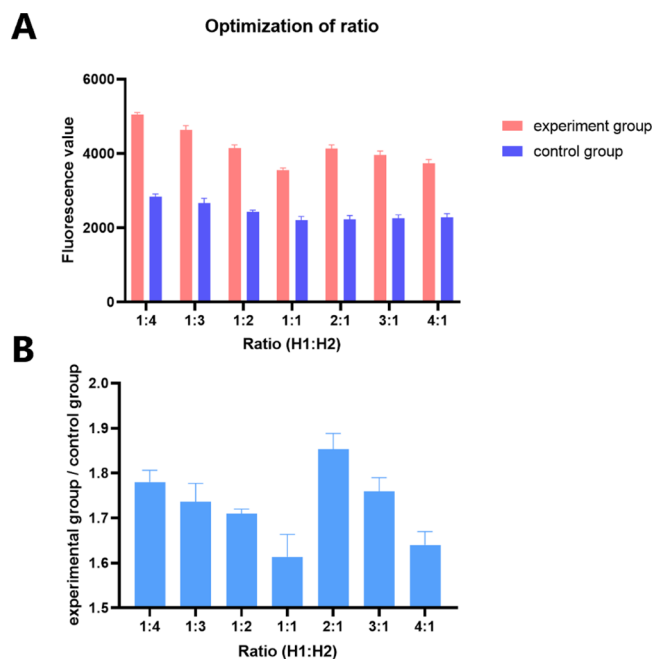


Figure 5. Proportion optimization by real-time fluorescence PCR. (A) Fluorescence values of different ratios and (B) fluorescence intensity ratio of the experimental group to the control group. In different ratios of H1 to H2 (H1/H2 = 1:4, H1/H2 = 1:3, H1/H2 = 1:2, H1/H2 = 1:1, H1/H2 = 2:1, H1/H2 = 3:1, and H1/H2 = 4:1), detecting the fluorescence values of the experimental group and the control group. Each value was derived from three independent detections, and the error bars mean standard deviations. When H1/H2 = 2:1, the fluorescence intensity ratio of the experimental group to the control group was the highest. The concentrations of H1, H2, and T are all 1 μ M.

nM, the ratio of fluorescence intensity between the experimental group and the control group was the highest.

3.5. Specificity of CHA-LFIA. Results as shown in Figure 7, the four tubes are, respectively, added with the Target, double base mutation sequence, single base mutation sequence, and buffer. The detection method of our study has high specificity, the single base mutation sequence can cause a significant decrease in the detection fluorescence value, and its fluorescence value is similar to the double mutation sequence. Both results are close to the blank control group.

3.6. Sensitivity of CHA-LFIA. The result is shown in Figure 8. At least the cutoff value was set with the mean value of the negative control fluorescence value plus three standard deviations. The fluorescence value of negative control is 56.20 ± 16.59 , and the cutoff value should be greater than or equal to 105.97. We set the cutoff value of the reaction to 106, and

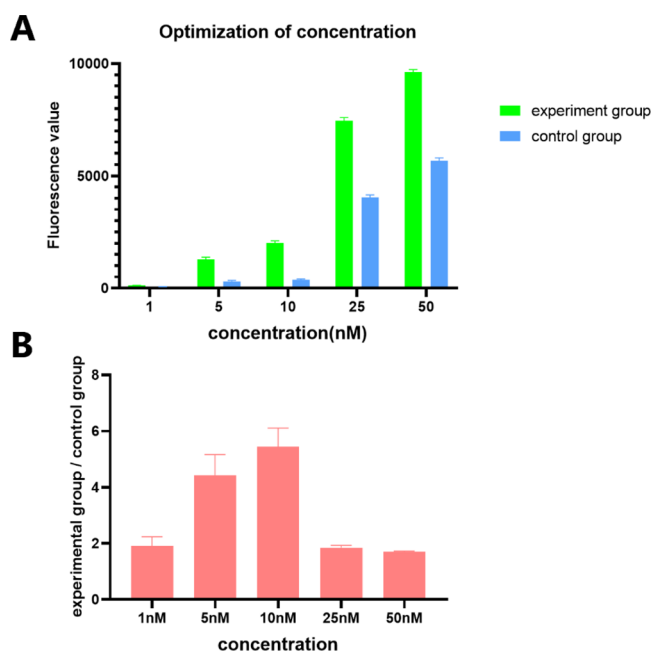


Figure 6. Concentration optimization. (A) Fluorescence values of different concentrations and (B) fluorescence intensity ratio of the experimental group to the control group. The fluorescence intensities were measured after added with different concentrations of H1 and H2 ranging from 1 to 50 nM in the presence of 100 pM target sequences. When H1 and H2 were 10 nM, the fluorescence intensity ratio of the experimental group to the control group reached the highest value. Error bars mean standard deviations that were calculated from four independent repeats.

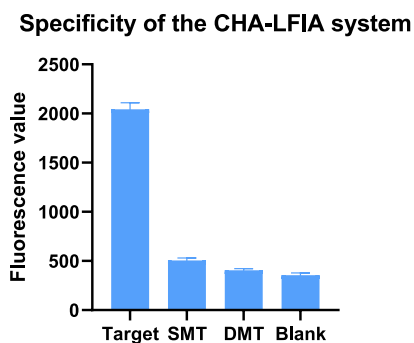


Figure 7. Specificity of CHA-LFIA. SMT: single mismatched target and DMT: double mismatched target. Each value was derived from four independent detections, and the error bars mean standard deviations. The fluorescence values of SMT and DMT are significantly different from the fluorescence values of the target.

those greater than 106 are considered to be positive samples. According to the cutoff value, the sensitivity of the detection method can reach 1 fM.

3.7. Detection of Clinical Samples. As shown in Figure 9, the average fluorescence value of vaginal secretions from 5 positive patients was 163.75 ± 57.79 , while that of 5 controls was 41.05 ± 10.31 . The fluorescence values of positive samples were significantly different from those of the control group ($P < 0.001$). According to the cutoff value, the results whose fluorescence value is greater than 106 are positive and those less than 106 are negative. After qualitative analysis, compared with the results of PCR detection, the consistency rate of the results reached 100%. This experiment shows that the

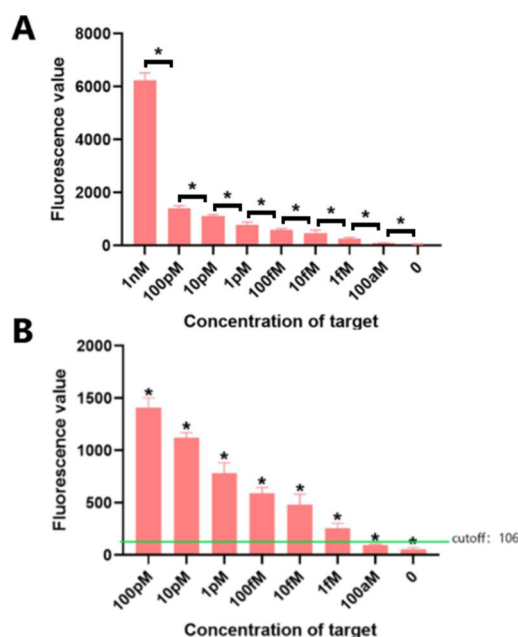


Figure 8. Sensitivity of CHA-LFIA. (A) Sensitivity of CHA-LFIA and (B) enlarge (A) in the range of 0 to 100 pM, and add cutoff value. *(independent *t*-test, $P < 0.05$) indicates significant difference from the respective former group. Each value was derived from ten independent detections, and the error bars mean standard deviations. The fluorescence value of negative control is 56.20 ± 16.59 , and the cutoff value is 106. According to the cutoff value, the sensitivity of the detection method can reach to 1 fM.

Clinical test

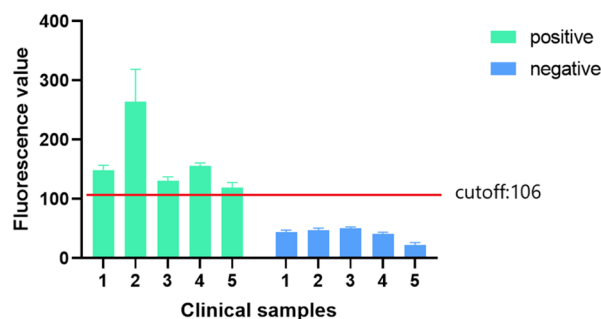


Figure 9. Detection of clinical samples. Each value was derived from four independent detections, and the error bars mean standard deviations. All results of positive samples exceed 106 and all results of negative samples cannot reach the cutoff value.

isothermal non-enzyme signal amplification system combined with the immunoassay strip can be used to detect clinical samples with *U. urealyticum*. To make negative controls, we have collected common pathogens of the genital tract in clinic for detection. We collected samples infected with *Neisseria gonorrhoeae*, *Mycoplasma genitalium*, and *Chlamydia trachomatis*. The number of each sample is 3. The result is shown in Figure 10. There is no cross reactivity between *U. urealyticum* and other common pathogens of the genital tract in clinic.

4. CONCLUSIONS

In this study, rapid, cheap, and sensitive methods for the detection of *U. urealyticum* was established. Combining the signal amplification of CHA reaction with the sensitivity of the lateral flow immunoassay test strip, *U. urealyticum* can be

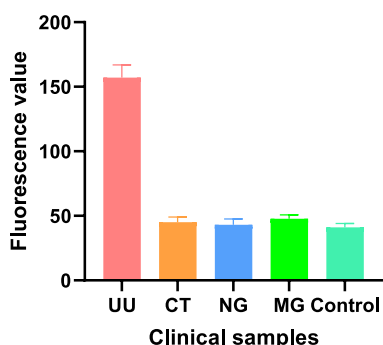


Figure 10. Detection of common pathogens of genital tract. UU: *U. urealyticum*; CT: *Chlamydia trachomatis*; NG: *Neisseria gonorrhoeae*; MG: *Mycoplasma genitalium*; and Control: Healthy people. Each value was derived from three independent detections, and the error bars mean standard deviations. The fluorescence values of *U. urealyticum* were significantly different from those of other common pathogens of the genital tract in clinic ($P < 0.01$). Moreover, P values between the control and CT, NG, and MG were all greater than 0.05.

detected accurately and quickly, and the results can be obtained within half an hour. Through the detection of clinical samples, its sensitivity and accuracy are verified, and it can reach the standard of clinical use. Because of the picky nature of *U. urealyticum*, it is difficult to identify and diagnose its infection in the clinical environment. Therefore, our further research will be valuable to improve the identification of infection and the treatment of inflammation. It can also ease the symptoms in advance and improve neonatal outcome.

■ ASSOCIATED CONTENT

SI Supporting Information

The Supporting Information is available free of charge at <https://pubs.acs.org/doi/10.1021/acsomega.2c02457>.

Native polyacrylamide gel electrophoresis for H1 and H2 hybridization induced by the target and the mismatched sequences (PDF)

■ AUTHOR INFORMATION

Corresponding Authors

Xiaobo Fan – Diagnostics Department, Medical School of Southeast University, Nanjing 210009, People's Republic of China; Email: 101011951@seu.edu.cn

Guoqiu Wu – Diagnostics Department, Medical School of Southeast University, Nanjing 210009, People's Republic of China; Zhongda Hospital, Center of Clinical Laboratory Medicine, Medical School, Southeast University, Nanjing 210009, People's Republic of China; Jiangsu Provincial Key Laboratory of Critical Care Medicine, Southeast University, Nanjing 210009, People's Republic of China; Email: nationball@163.com

Authors

Feng Xiao – Diagnostics Department, Medical School of Southeast University, Nanjing 210009, People's Republic of China; orcid.org/0000-0002-2139-5094

Qingrong Qu – Department of Tuberculosis, Shanghai Pulmonary Hospital, School of Medicine, Tongji University, Shanghai 200433, China

Mingyuan Zou – Diagnostics Department, Medical School of Southeast University, Nanjing 210009, People's Republic of China

Feiya Su – Diagnostics Department, Medical School of Southeast University, Nanjing 210009, People's Republic of China

Huina Wu – Diagnostics Department, Medical School of Southeast University, Nanjing 210009, People's Republic of China; orcid.org/0000-0002-4834-3040

Yan Sun – Diagnostics Department, Medical School of Southeast University, Nanjing 210009, People's Republic of China

Meiling Zhou – Diagnostics Department, Medical School of Southeast University, Nanjing 210009, People's Republic of China

Fengfeng Zhao – Diagnostics Department, Medical School of Southeast University, Nanjing 210009, People's Republic of China; Zhongda Hospital, Center of Clinical Laboratory Medicine, Medical School, Southeast University, Nanjing 210009, People's Republic of China

Yuming Yao – Diagnostics Department, Medical School of Southeast University, Nanjing 210009, People's Republic of China

Gulinaizhaer Abudushalamu – Diagnostics Department, Medical School of Southeast University, Nanjing 210009, People's Republic of China

Yaya Chen – Diagnostics Department, Medical School of Southeast University, Nanjing 210009, People's Republic of China

Chen Zhang – Zhongda Hospital, Center of Clinical Laboratory Medicine, Medical School, Southeast University, Nanjing 210009, People's Republic of China

Complete contact information is available at:

<https://pubs.acs.org/10.1021/acsomega.2c02457>

Author Contributions

[†]F.X. and Q.Q. contributed equally to this article as first authors.

Notes

The authors declare no competing financial interest.

■ ACKNOWLEDGMENTS

This project was supported by the National Science and Technology Major Project (no. 2020ZX09201015) and the National Natural Science Foundation of China (no. 81773624 and 81603016).

■ REFERENCES

- (1) Kokkayil, P.; Dhawan, B. Ureaplasma: current perspectives. *Indian J. Med. Microbiol.* **2015**, *33*, 205–214.
- (2) Zheng, W.-W.; Zhang, W.-J.; Cui, D.; Nie, Z.-C.; Ding, B.-S.; Cheng, J.-H.; Mei, C.-Z. Examination of Ureaplasma urealyticum and Mycoplasma hominis in 4082 Chinese patients. *Braz. J. Med. Biol. Res.* **2020**, *54*, No. e10099.
- (3) Cai, S.; Pan, J.; Duan, D.; Yu, C.; Yang, Z.; Zou, J. Prevalence of Ureaplasma urealyticum, Chlamydia trachomatis, and Neisseria gonorrhoeae in gynecological outpatients, Taizhou, China. *J. Clin. Lab. Anal.* **2020**, *34*, No. e23072.
- (4) Zhang, Q.; Xiao, Y.; Zhuang, W.; Cheng, B.; Zheng, L.; Cai, Y.; Zhou, H.; Wang, Q. Effects of biovar I and biovar II of ureaplasma urealyticum on sperm parameters, lipid peroxidation, and deoxyribonucleic acid damage in male infertility. *Urology* **2014**, *84*, 87–92.
- (5) Zhu, X.; Li, M.; Cao, H.; Yang, X.; Zhang, C. Epidemiology of and in the semen of male outpatients with reproductive disorders. *Exp. Ther. Med.* **2016**, *12*, 1165–1170.

- (6) Sprong, K. E.; Mabenge, M.; Wright, C. A.; Govender, S. species and preterm birth: current perspectives. *Crit. Rev. Microbiol.* **2020**, *46*, 169–181.
- (7) Beeton, M. L.; Payne, M. S.; Jones, L. The Role of spp. in the Development of Nongonococcal Urethritis and Infertility among Men. *Clin. Microbiol. Rev.* **2019**, *32*, 001377.
- (8) Capoccia, R.; Greub, G.; Baud, D. *Ureaplasma urealyticum*, *Mycoplasma hominis* and adverse pregnancy outcomes. *Curr. Opin. Infect. Dis.* **2013**, *26*, 231–240.
- (9) Brown, M. B.; Cassell, G. H.; Taylor-Robinson, D.; Shepard, M. C. Measurement of antibody to *Ureaplasma urealyticum* by an enzyme-linked immunosorbent assay and detection of antibody responses in patients with nongonococcal urethritis. *J. Clin. Microbiol.* **1983**, *17*, 288–295.
- (10) Liepmann, M. F.; Wattle, P.; Dewilde, A.; Papierok, G.; Delecour, M. Detection of antibodies to *Ureaplasma urealyticum* in pregnant women by enzyme-linked immunosorbent assay using membrane antigen and investigation of the significance of the antibodies. *J. Clin. Microbiol.* **1988**, *26*, 2157–2160.
- (11) Fuwa, K.; Seki, M.; Hirata, Y.; Yanagihara, I.; Nakura, Y.; Takano, C.; Kuroda, K.; Hayakawa, S. Rapid and simple detection of *Ureaplasma* species from vaginal swab samples using a loop-mediated isothermal amplification method. *Am. J. Reprod. Immunol.* **2018**, *79*, No. e12771.
- (12) Huang, Y.; Pan, H.; Xu, X.; Lv, P.; Wang, X.; Zhao, Z. Droplet digital PCR (ddPCR) for the detection and quantification of *Ureaplasma* spp. *BMC Infect. Dis.* **2021**, *21*, 804.
- (13) Sun, Z.; Meng, J.; Wang, S.; Yang, F.; Liu, T.; Zeng, X.; Zhang, D.; Zhu, H.; Chi, W.; Liu, Y.; et al. A New Multiplex Genetic Detection Assay Method for the Rapid Semi-Quantitative Detection of Six Common Curable Sexually Transmitted Pathogens From the Genital Tract. *Front. Cell. Infect. Microbiol.* **2021**, *11*, 704037.
- (14) Yin, P.; Choi, H. M. T.; Calvert, C. R.; Pierce, N. A. Programming biomolecular self-assembly pathways. *Nature* **2008**, *451*, 318–322.
- (15) Gao, M.; Waggoner, J. J.; Hecht, S. M.; Chen, S. Selective Detection of Dengue Virus Serotypes Using Tandem Toehold-Mediated Displacement Reactions. *ACS Infect. Dis.* **2019**, *5*, 1907–1914.
- (16) Gao, M.; Daniel, D.; Zou, H.; Jiang, S.; Lin, S.; Huang, C.; Hecht, S. M.; Chen, S. Rapid detection of a dengue virus RNA sequence with single molecule sensitivity using tandem toehold-mediated displacement reactions. *Chem. Commun.* **2018**, *54*, 968–971.
- (17) Zou, M.; Su, F.; Zhang, R.; Jiang, X.; Xiao, H.; Yan, X.; Yang, C.; Fan, X.; Wu, G. Rapid point-of-care testing for SARS-CoV-2 virus nucleic acid detection by an isothermal and nonenzymatic Signal amplification system coupled with a lateral flow immunoassay strip. *Sens. Actuators, B* **2021**, *342*, 129899.
- (18) Su, F.; Zou, M.; Wu, H.; Xiao, F.; Sun, Y.; Zhang, C.; Gao, W.; Zhao, F.; Fan, X.; Yan, X.; et al. Sensitive detection of hepatitis C virus using a catalytic hairpin assembly coupled with a lateral flow immunoassay test strip. *Talanta* **2022**, *239*, 123122.
- (19) Wu, H.; Zou, M.; Fan, X.; Su, F.; Xiao, F.; Zhou, M.; Sun, Y.; Zhao, F.; Wu, G. Facile, Rapid, and Low-Cost Detection for Influenza Viruses and Respiratory Syncytial Virus Based on a Catalytic DNA Assembly Circuit. *ACS Omega* **2022**, *7*, 15074–15081.